JOURNAL OF PHYSICAL ORGANIC CHEMISTRY, VOL. 10, 311–322 (1997)

ENANTIOSELECTIVE BINDING IN GAS CHROMATOGRAPHY: A COMPUTATIONAL STUDY OF CHIRAL SELECTION BY PERMETHYL-β-CYCLODEXTRIN

KENNY B. LIPKOWITZ,* BOB CONER, MICHAEL A. PETERSON AND ANTONIO MORREALE

Department of Chemistry, Indiana University Purdue University at Indianapolis, 402 North Blackford Street, Indianapolis, Indiana 46202, USA

Stochastic molecular dynamics simulations were used to determine the enantiomer retention orders of moderately polar analytes binding to permethylated β-cyclodextrin, a popular chiral stationary phase used in gas chromatography. It is found that averaging over multiple trajectories, each of which are lengthy, is required to faithfully reproduce experiment. From the simulations we find the major binding domain to be the interior of the macrocycle rather than the exterior with most analytes having a preference for associating to the primary rim rather than to the secondary rim. It is also found that the intermolecular forces responsible for holding the complexes together are the short range dispersion forces, and that the enantiodifferentiating forces of the competing diastereomeric complexes are dominated by the van der Waals contributions to the intermolecular energy. © 1997 by John Wiley & Sons, Ltd.

J. Phys. Org. Chem. **10**, 000–000 (1997) No. of Figures: 7 No. of Tables: 6 No. of References: 23

Keywords: enantioselective binding; gas chromatography; chiral selection; permethyl-β-*cyclodextrin*

Received 2 October 1996; accepted 15 November 1996

INTRODUCTION

Compelling reasons exist for the separation of enantiomers, and to accomplish this task, major advances have been made during the last 10 years in the area of chiral chromatography.[1] Rather than converting enantiomers in to diastereomers *in situ* followed by chromatographic separation and reconversion to the resolved enantiomers (an 'indirect' method), many scientists prefer the 'direct' approach of chiral chromatography. Here the enantiomeric analytes pass through a chromatographic column forming transient diastereomeric complexes that, by virtue of their different association constants, give rise to different retention times. The advantages of chiral chromatography are such that a wide range of methods have been developed for these direct resolutions. For all these methods the underlying requirement is that they possess some sort of chiral environment, although in some instances one can achieve partial resolution of enriched mixtures on non-chiral columns.[2]

A large number of chiral stationary phases exist, most of which are adsorbed or directly tethered to inert silica that is then packed into the column. These CSPs are derived from a wide range of materials, including natural and non-natural sources. Because these materials are so diverse in both their properties as well as how they form the transient complexes, Wainer[3] has suggested classifying them based on their mechanism of complexation. One category, Type III CSPs, act by host–guest complexation. The best example of this class of CSP, and also the most widely used Type III CSP, are the cyclodextrins and their derivatives. They are used in planar,[4] gas,[5] liquid[6] and super-/subcritical fluid chromatography.[7] Cyclodextrins have also been extensively studied because of their ability to form host–guest complexes of interest to physical organic chemists,[8] but also because their chiral microenvironments are suitable as enzyme mimics,[9] and microenvironments for asymmetric synthesis.[10] Clearly, then, there exist a wide range of scientists[11] and technologists[12] who are interested in this class of compounds for a variety of reasons. Understanding how these macrocycles work as chiral selectors is therefore important.

Our focus is on permethylated β-cyclodextrin, **1**, as a host molecule because it is the most commonly used CSP in gas chromatography. Moreover, the binding and discrimination in this type of chromatography are in the 'gas' phase rather than an aqueous medium where hydrophobic forces are known to induce host–guest complexation. Figure 1 depicts the structure of this inherently chiral macromolecule.

* *Correspondence to*: K. B. Lipkowitz. E-mail: lipkowitz@chem.iupui.edu.

Contract grant sponsor: National Science Foundation; *Contract grant number:* CHE 9412512.

© 1997 by John Wiley & Sons, Ltd. CCC 0894–3230/97/050311–12 $17.50

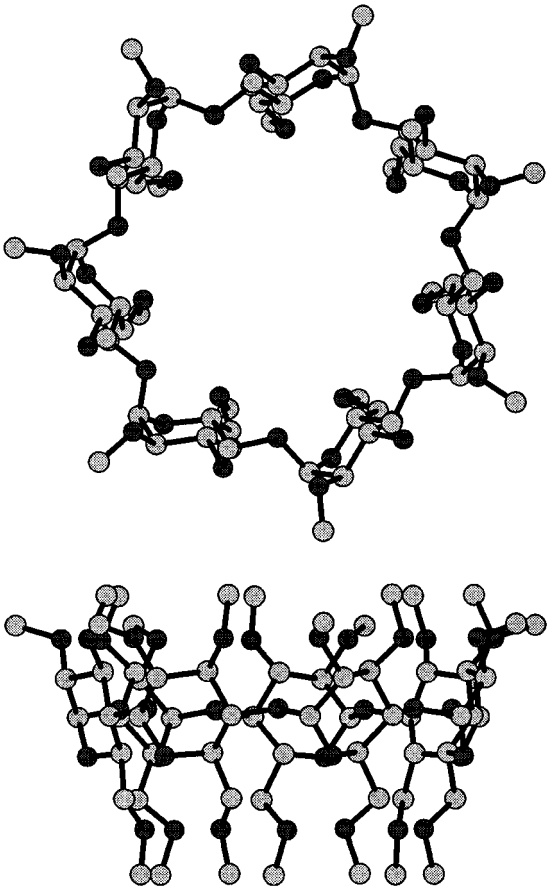

Figure 1. (Top) view looking into the permethyl-β-cyclodextrin chiral cavity. (Bottom) side view illustrating the typical conical shape of these molecules. The more open end is the 2° rim and the narrower end is the 1° rim. Dark gray tones represent oxygen atoms and light gray tones are carbons. Hydrogen atoms omitted for clarity. Structure presented as having a sevenfold symmetric, time-averaged geometry

The key issue we address here is where binding takes place, and in particular whether binding occurs inside or outside of the CD cavity. Berthod *et al.*[13] have recently presented their results of a lengthy extrathermodynamic study of gas-phase bindings using a wide range of analytes on similar CSPs and found evidence for two binding modes. One mode presumably corresponds to encapsulation (interior binding) and the other to exterior binding. We now focus on the binding of low molecular weight compounds to the permethylated β-cyclodextrin **1** to answer three fundamental questions: first, where in or around the macrocycle do guests tend to bind?; second, what are the intermolecular forces responsible for holding the diastereomeric complexes together?; and third, what are the intermolecular forces responsible for chiral discrimination? In this paper, we present the results of molecular dynamics simulations of several analytes binding to **1** so that we can assess where small, moderately polar guests tend to bind in the gas phase as well as to understand the origins of enantioselection.

COMPUTATIONAL TOOLS

Molecular mechanics[14] calculations were carried out with the AMBER* force field[15] as found in Macromodel 5·5.[16] The PR conjugate gradient minimizer[17] was used to minimize the energies, and convergence was obtained when the gradient root mean square was below 10^{-3} kJ mol^{-1} Å^{-1}. Throughout this paper all force field calculations assume a dielectric of 1·0, and no cut-offs of any kind were used.

Stochastic dynamics[18] (SD) simulations were carried out with the AMBER* force field with the fully optimized, lowest energy structures as the initial structures. The analyte–CD complexes were warmed to the simulation temperature over a period of 5 ps, then equilibrated for 25 ps. During the production simulations of 5000 ps each, structures were saved the disk every 0·5 ps, resulting in 10 000 saved structures from each trajectory. The SD simulation each had a time step of 0·5 fs with equilibration and production run temperatures of 353 K (analyte **2**),[19] 370 K (analyte **3**)[20] and 383 K (analyte **4**)[21] to be consistent with experimental gas chromatographic conditions. Translational and rotational momentums were removed every 100 time steps. To keep the CD–analyte complexes together, flat-bottom restraints were used between the stereogenic center of the analyte and the linking acetal oxygens of the CD [flat-bottom restrains allow the selected degree of freedom, a distance from the cyclodextrins acetal oxygens in this case, to move freely a desired distance (20 Å) before a harmonic constraining force is applied; the restraining force constant was set equal to 100 kJ mol^{-1} Å^{-1}]. Using these restraints, if the analyte strayed more than 20 Å away from any linking acetal oxygen, it was gently pushed back towards the CD. These restraints were used in the heating, equilibration and production portions of the simulations.

Post-simulation analysis of the SD trajectories was performed with an in-house program which computes, among other things, intermolecular energies (using the AMBER* force field in this case) and the center of mass positions of a molecule relative to another (anout, written by MAP to analyze MacroModel molecular dynamics trajectories; this software is available from Dr M. A. Peterson, Department of Chemistry, University of Florida, Gainesville, FL 32611, USA). In this work the analyte's positions were calculated relative to the centroid of the best-fit plane through the acetal linking oxygens of the CD. For trajectories being averaged, these analyte positions were combined and placed on a three-dimensional grid. The sides connecting eight adjacent grid points define a volume element. The number of analyte positions in each volume element is tallied and the resulting number densities are output in a form suitable for visualization with

© 1997 by John Wiley & Sons, Ltd.

IRIS Explorer [IRIS Explorer Center (North America), Downers Grove, IL 60551–5702, USA, or via <URL http://www.nag.co.uk/1h/Welcome_IEC>]. This allows us to identify where the analytes prefer to bind to the CD (see below).

SIMULATION STRATEGY

What we wish to accomplish is to stimulate the binding of enantiomeric analytes to CSP molecules as those analytes migrate through the chromatographic column. It is not possible to do this computationally given the current tools we have to work with. How, then, can one sample the various intermolecular interactions between analyte and CSP? The approach we take is to use a single CSP molecule with a single analyte molecule and carry out molecular dynamics simulations on those systems. In reality the analyte molecule binds to the CD but then dissociates and moves downstream to another CD, where it again binds. The enantioseparation that we are interested in predicting depends on the differential binding energies. To effect this simulation with a single selector (the CSP) and a single selectand (analyte), we allow the molecules to bind, dissociate and re-bind multiple times by placing a reflective wall around the diastereomeric complexes. To accomplish this we use a flat-bottom potential having no restraining forces until the analyte molecule moves 20 Å from the cyclodextrin. At that point a 100 kJ mol^{-1} $Å^{-1}$ restraining force is applied which pulls the analyte back toward the CSP where it can further associate. Effectively, then, what we have accomplished in this way is to allow the analyte to collide randomly with the CSP in all possible conformations, orientations and positions as it would in the real system.

To probe the system fully we need to sample as large a volume of phase space for each diastereomeric complex as possible. Moreover, to ensure that no computational artifacts are introduced into the system, e.g. starting the *R* enantiomers trajectory on one rim of the cavity and the *S* enantiomers on the other rim or one enantiomer inside the cavity with the other on the outside, we superimpose selected atoms of each enantiomer to generate a racemic 'supermolecule' that is then placed in specified starting positions (see figure 2). Once both enantiomers have been docked in the same place and with the same orientation/conformations, one of the enantiomers is removed, leaving behind a well defined binary, diastereomeric complex with the desired stereochemistry.

The initial docking positions are illustrated in Figure 2. In this cartoon the cyclodextrin is represented by a truncated conical cylinder and the asterisks correspond to the location of the analyte (note that because the 'supermolecule' has been docked, one is assured of the same initial positions and orientations for both enantiomers for each trajectory being computed). The wide end of the cyclodextrin is the secondary rim and the narrower one the primary rim.

Five trajectories are run for each enantiomer beginning from the five initial positions illustrated in Figure 2. For docking purposes the cyclodextrin used is a sevenfold symmetric structure that allows us to place the analytes at precise positions parallel or perpendicular to the sevenfold axis. The reader should note that cyclodextrins are not symmetric at any given time. They are inherently flexible and undergo wide-amplitude flexing motions.[22] Over a long enough simulation time, however, the time-averaged CD structure is expected, and found, to be nearly symmetric (see below). The symmetric structure is used only for docking purposes.

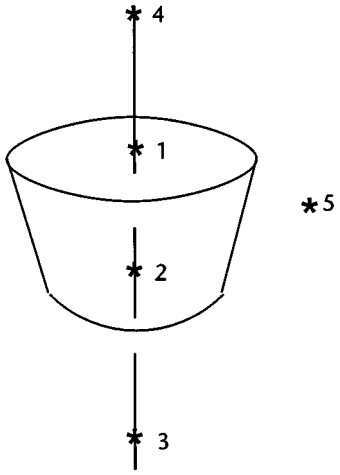

Figure 2. Cartoon illustrating the starting points of the five trajectories for both *R* and *S* enantiomers of all analytes. The conical bucket shape represents the cyclodextrin depicted in Figure 1. The asterick labels correspond to the specific trajectory number described throughout the text

The upshot of our simulation strategy is to sample a wide volume of phase space beginning from different initial conditions corresponding to different locations on the complexes' potential hypersurface. We then run very long simulations (5 ns for each trajectory), generating an ensemble of trajectories whose energies are then averaged. At this point we need to ask ourselves whether or not we are artificially biasing our results. One bias involves placing the analyte into the CD (if trapped within the cavity the energies will be unfairly weighted to represent internal binding, an issue we are investigating here). To illustrate that the simulations are not artifically biased toward internal binding, Figure 3 shows the location of the analyte (its center of mass more specifically) with respect to the host. The data in Figure 3 corresponds to a single trajectory of analyte **2** beginning from the interior of the host. The time period this data was collected over is from 0–500 ps of the production part of the simulation (recall each of our trajectories is 5 ns). From the figure we see that the analyte quickly escapes from the interior of themacrocycle and begins to sample sites at the exterior of the host. Similar plots with the analyte beginning outside the CD show the analytes likewise move

© 1997 by John Wiley & Sons, Ltd.

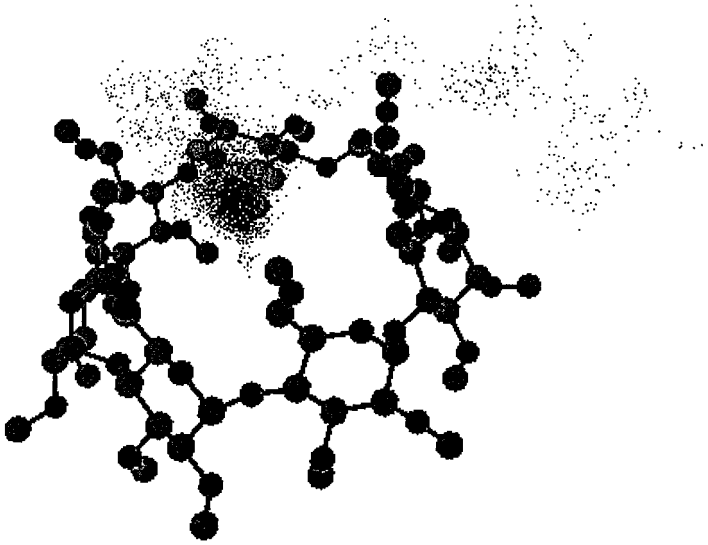

Figure 3. The first 10% of pinene trajectory 1 (see figure 2) illustrating that molecules quickly escape from the interior of the CD cavity. The dots correspond to the pinene's center of mass relative to the cyclodextrin

around and begin to sample the inside of the CD cavity, indicating, as we shall see later, that the intermolecular potential energy surfaces of these weakly bound complexes are very shallow, allowing rapid migration into and out of the macrocycle. Accordingly, the simulation strategy we adopt here seems not to be biased and is set up in a way so as to explore as much of phase space as possible in an evenhanded way.

RESULTS

The analytes considered in this study are representative of moderately polar compounds that have been resolved on permethylated cyclodextrin CSPs. Compounds **2** and **3** are hydrocarbons lacking any sort of polar functionality while the analyte **4** is moderately polar with the carbon–fluorine bond capable of dipolar associations with various ether and acetal linkages of the CD. In all cases the analytes have been resolved on **1**, albeit by different groups and at different chromatographic temperatures and flow rates.[19–21]

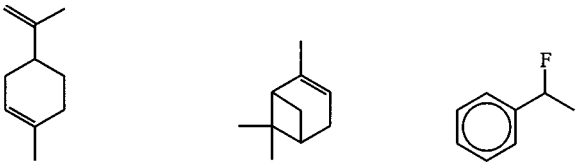

2 **3** **4**

The results of our simulations are presented in Tables 1–3. Both the total potential energies for each trajectory as well as the component force field energies for each trajectory are given. The averages are presented at the bottom of each table. R1, R2, etc. corresponds to the trajectories 1, 2, etc., for the R enantiomer while the designation S1, S2, etc. are those trajectories for the S enantiomer. Experimentally, in all cases, the R enantiomer is eluted from the column after the S enantiomer.[26] In our tables one sees that the R enantiomer of limonene, α-pinene and 1-fluorophenylethane all have the lower averaged potential energies compared to their enantiomeric counterparts meaning they are more tightly affixed to the CSP and, accordingly, are predicted to be longer retained on the chromatographic column. Hence the computed retention orders agree fully with experimental retention orders. The differences in energy for each enantiomeric set are very small, but this too is what one finds experimentally. The energies presented in the tables are not true free energies because the entropies have not been determined explicitly. Thus direct comparisons with chromatographic α values (the ratio of chromatographic capacity factors, related to free energy differences) cannot be made. Nonetheless, the magnitudes of these energy differences taken together with the correct retention orders indicate that our simulations are virtuous and that we can now begin to extract meaningful data from those simulations.

DISCUSSION

Before discussing the binding sites and origins of enantioselection, it is imperative to point out that very long simulation times, along with averaging over multiple

© 1997 by John Wiley & Sons, Ltd.

Table 1. MD results (kJ mol^{-1}) for limonene–CD

	Total	Stretch	Bend	Torsion	vdW	Electrostatic
*R*1	1767·66	382·70	595·76	290·26	45·23	453·66
*R*2	1783·51	383·24	595·42	303·29	46·83	455·73
*R*3	1781·82	383·47	599·92	286·39	57·62	454·42
*R*4	1784·81	383·49	603·06	283·16	61·19	453·91
*R*5	1779·12	383·51	601·90	285·00	58·35	450·36
Av. E_R	1779·38	383·08	599·21	289·62	53·85	453·62
*S*1	1779·50	383·44	598·73	286·27	59·60	451·46
*S*2	1778·58	382·97	599·48	286·66	58·60	450·87
*S*3	1796·46	382·87	598·98	300·47	58·99	455·15
*S*4	1793·03	383·23	602·02	294·14	61·61	452·03
*S*5	1783·44	383·16	602·71	290·90	57·92	448·75
Av· E_S	1786·20	383·13	600·38	291·69	59·34	451·65
$\Delta\Delta E_{R-S}$	−6·82	−0·05	−1·17	−2·07	−5·49	1·96

trajectories, are required to obtain the correct chromatographic retention orders. Presented in Figure 4, as an example, are running averages of the total potential energies for the five trajectories for *R* and *S* enantiomers of α-pinene.

[Note that pinene has two stereogenic centers and should more properly be named using two CIP stereochemical designators or as (+)- or (−)-antipodes; however, most chromatography papers designate the (−)-antipode as *S* and

Table 2. MD results (kJ mol^{-1}) for pinene–CD

	Total	Stretch	Bend	Torsion	vdW	Electrostatic
*R*1	1881·88	385·43	666·37	324·36	71·51	434·31
*R*2	1868·59	385·36	666·50	316·54	67·49	432·70
*R*3	1876·51	385·70	667·67	314·53	73·26	435·35
*R*4	1873·36	385·82	667·07	310·69	73·99	435·80
*R*5	1860·20	385·19	664·10	328·01	47·87	435·03
Av. E_R	1872·11	385·50	666·34	318·81	66·82	434·64
*S*1	1874·76	385·82	666·27	315·10	72·60	434·97
*S*2	1866·02	385·48	666·27	318·38	62·50	433·39
*S*3	1883·07	385·48	667·48	323·52	74·21	433·18
*S*4	1885·78	385·26	665·28	326·10	73·93	435·21
*S*5	1866·38	386·07	669·90	305·88	69·39	435·14
Av. E_S	1875·36	385·62	667·04	317·80	70·53	434·38
$\Delta\Delta E_{R-S}$	−3·25	−0·12	−0·57	1·01	−3·70	0·26

Table 3. MD results (kJ mol^{-1}) for 1-fluorophenylethane–CD

	Total	Stretch	Bend	Torsion	vdW	Electrostatic
*R*1	1904·63	369·67	566·61	510·56	31·84	425·95
*R*2	1903·98	369·75	566·04	511·17	21·98	427·04
*R*3	1918·67	370·76	572·73	500·32	50·83	424·03
*R*4	1924·43	370·17	569·47	509·52	48·81	426·46
*R*5	1920·68	369·70	568·05	510·07	46·48	426·38
Av. E_R	1912·93	370·01	568·58	508·33	41·59	425·97
*S*1	1904·18	369·49	565·24	511·46	30·79	427·70
*S*2	1917·63	370·65	571·97	500·75	50·52	423·79
*S*3	1905·39	369·76	567·58	510·69	31·69	425·67
*S*4	1926·71	370·23	569·74	509·44	48·82	428·48
*S*5	1906·38	369·06	564·39	512·20	33·08	427·65
Av. E_S	1913·49	369·84	567·78	508·91	38·98	426·56
$\Delta\Delta E_{R-S}$	−0·56	0·17	0·80	−0·58	2·61	−0·59

© 1997 by John Wiley & Sons, Ltd.

the (+)-antipode as *R*, referring only to the stereocenter at C1. To be consistent with the chromatographic literature we adopt that simpler nomenclature scheme.] If one were to use the data from a single trajectory, even if it were lengthy, the predicted retention order could be incorrectly assigned depending on which trajectory was used, e.g. trajectories 1 and 2. Likewise, even if one were to average over multiple trajectories, by using traditional simulation times of 500–1000 ps could also lead one to predict the incorrect retention orders. To be successful in making predictions we find that the number of trajectories and the duration of each trajectory should be at least those which are presented in this paper, otherwise one runs the risk of improper sampling of phase space and, consequently, predicting the wrong elution orders. Our comment concerning the number and duration of trajectories is based on previous, unpublished experience. It is imperative that we predict correct retention orders consistently for all analytes before we extract information from those simulations. Earlier we carried out molecular simulations using multiple trajectories, each of which was only 500 ps long, a standard time value found in the literature. While most results were predicted correctly using that computational protocol, several inverted retention orders were predicted. Similarly, we attempted using a

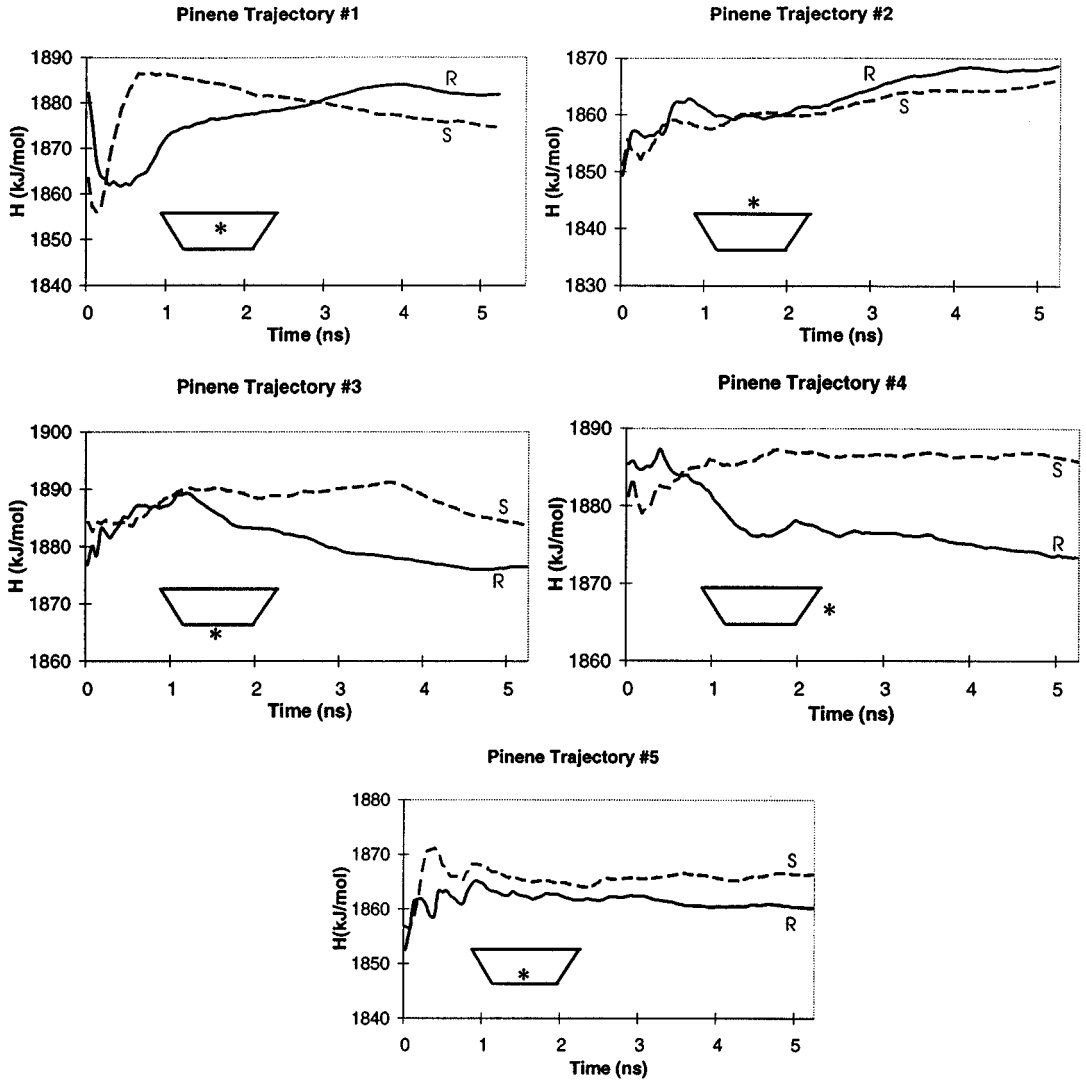

Figure 4. Running averages of potential energies for the five (*R/S*)-pinene trajectories illustrating that averaging over long, multiple trajectories is required to predict correctly analyte retention orders

© 1997 by John Wiley & Sons, Ltd.

simulation protocol having a single, lengthy trajectory, but that too resulted in several incorrect predictions. However, combining long times with multiple trajectories appears to be a reliable computational protocol for consistently giving correct answers. Hence our suggestion that the number and duration of trajectories be similar to those described in this paper is based on past experience. Finally, the reader should note that extending the simulation times might lead to incorrect answers. We did not bias the outcome of these results by deliberately stoping the simulation times at 5 ns so as to be consistent with experiment. Rather, that time was arbitrarily selected so as to be long, but not too long to be intractable given our computing resources.

We now turn our attention to enantioselective binding. The first issue we address concerns the preferred binding site of the analytes. In particular we ask whether analytes prefer to bind on the interior or the exterior of the CD cavity. This is an extremely controversial issue amongst separation scientists. To answer this question we placed the time-averaged CDs center of mass at the origin of a Cartesian coordinate system which in turn was placed on a grid. Eight neighboring grid points constitute a small volume element (a volumetric pixel or a 'voxel'). The number of times an analyte's center of mass passed through

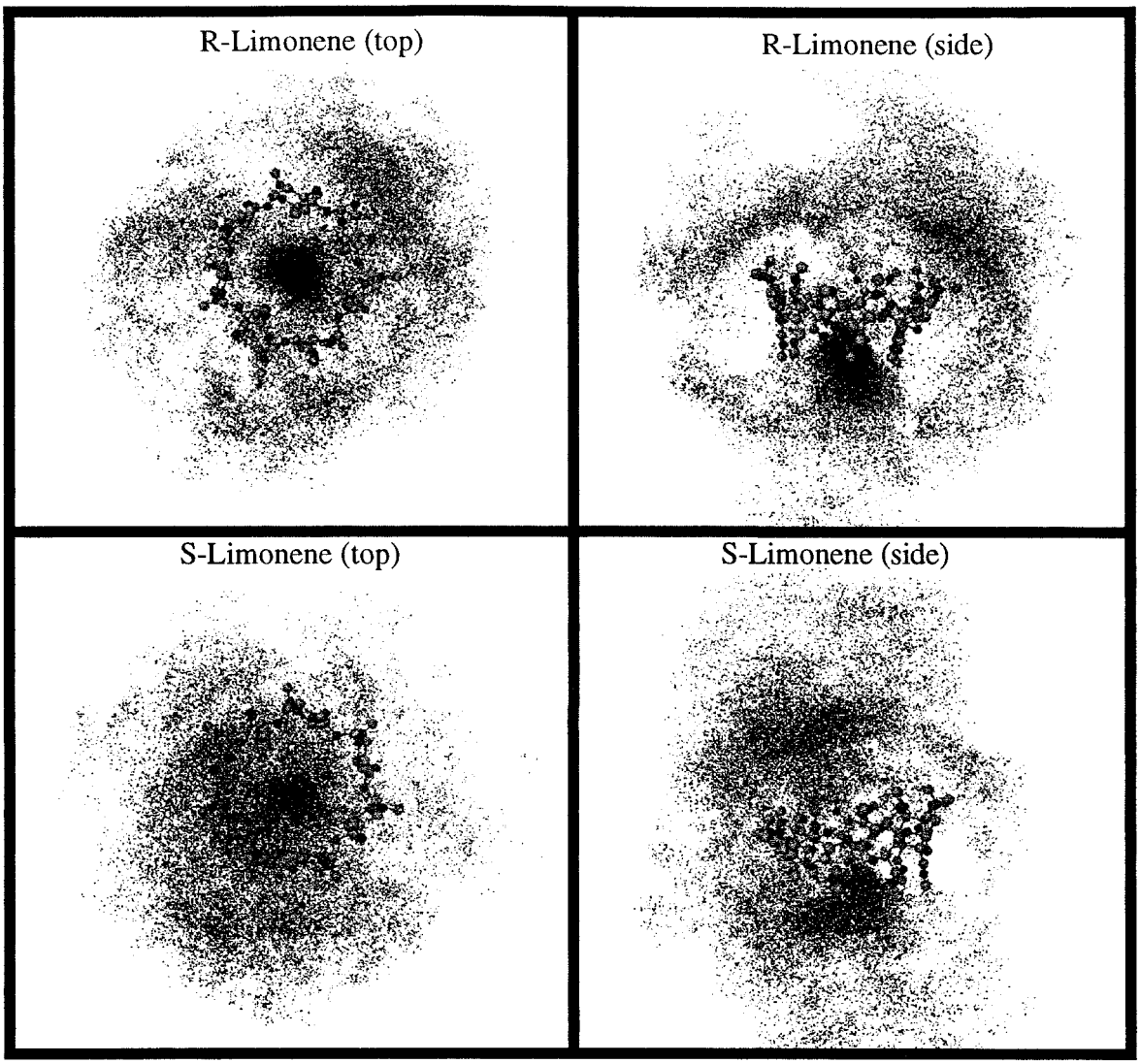

Figure 5. 'Dot plot' illustrating the limonene center of mass, relative to the cyclodextrin, over the combined 25 ns simulation. (Top end-on and side views of the *R* enantiomer; (bottom) end-on and side views of the *S* enantiomer

© 1997 by John Wiley & Sons, Ltd.

a particular voxel, evaluated over the entire simulation time period, was tallied. The most densely populated volume elements are the preferred binding sites. To visualize this Figures 5–7 show the locations of analytes **2**–**4** over the course of the simulation.

It is evident from Figures 5–7 that all analytes prefer to bind to the interior of the CD cavity. The reason for this behavior is that interior binding is stabilized by the macrocycle which collapses around these small analytes, thus maximizing van der Waals forces (in contrast to exterior binding). One also notes, in general, that the more tightly bound *R* substrates have better defined binding sites than do the less tightly bound *S* enantiomers, which appear more scattered. It is also instructive to note that preference is given for all analytes to bind to the primary rim of the macrocycle but this must be stated with some trepidation because in some instances, e.g. (*S*) limonene, it is difficult to discern which rim is more heavily populated. This is to be contrasted with the results of most aqueous phase NMR studies where intermolecular NOEs indicate a preference for the wider, secondary rim.[23] Generally, however, at these elevated gas chromatographic conditions the analyte is rapidly sliding back and forth between the two rims as well as into and out of the cavity itself. Still, clear preference is

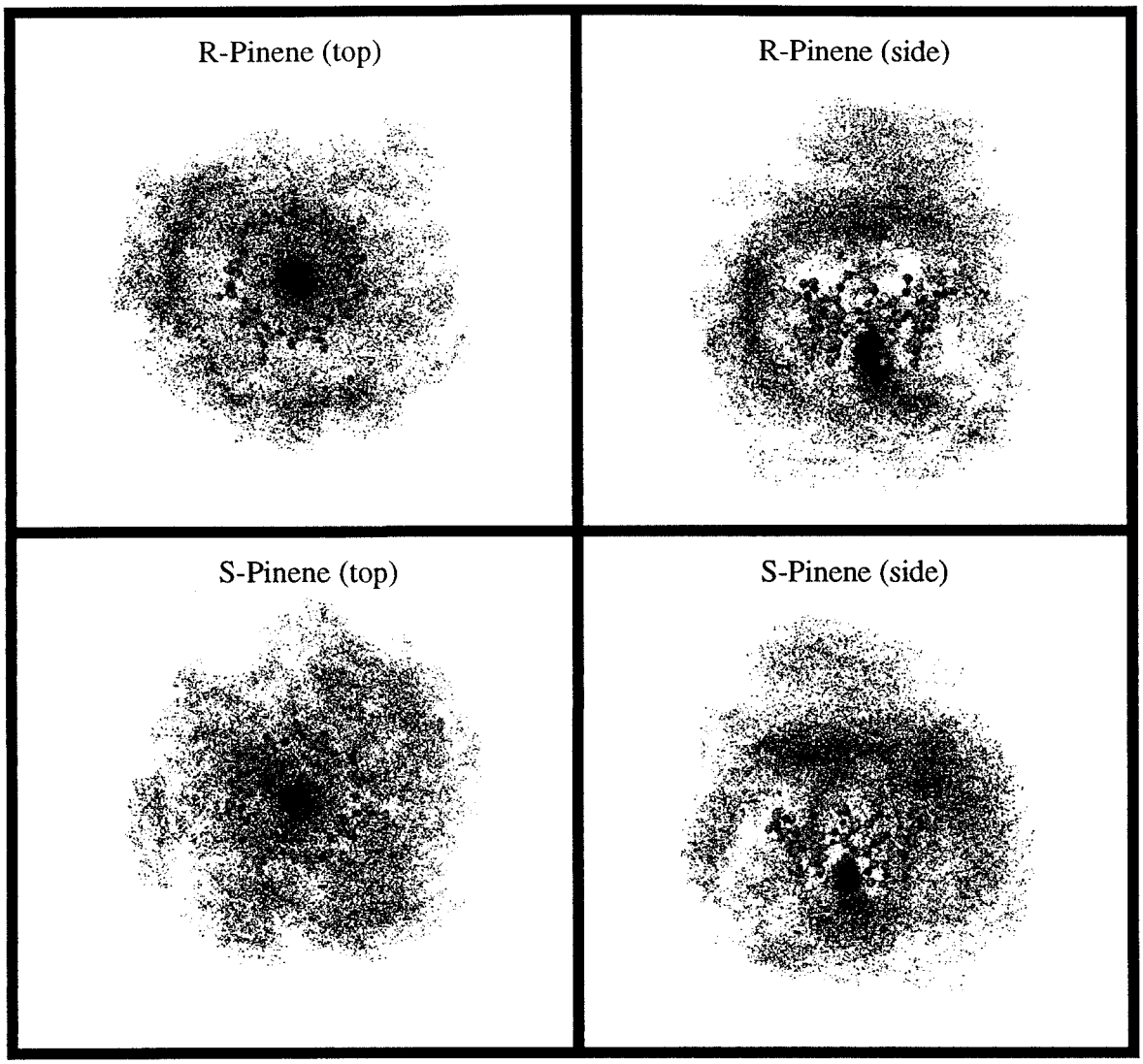

Figure 6. 'Dot plot' illustrating the pinene center of mass, relative to the cyclodextrin, over the combined 25 ns simulation. (Top) end-on and side views of the *R* enantiomer; (bottom) end-on and side views of the *S* enantiomer

© 1997 by John Wiley & Sons, Ltd.

noted for interior binding rather than exterior binding, and there exists a propensity for analytes to associate with the more flexible primary rim of the cavity rather than the secondary rim.

The next issue we address concerns the forces responsible for host–guest complexation. To evaluate this we must not consider the energies in Tables 1–3 because those values include the interaction energies between host and guest molecules in addition to the internal self-energies of both molecules. More appropriate for our discussion are the intermolecular energies only. These energies can be decomposed into short-range dispersion components and long-range electrostatic components.

These intermolecular contributions are compiled in Tables 4–6, for each trajectory, as well as for the full 25 ns simulations. For the hydrocarbon examples one expects, and finds, a relatively small intermolecular electrostatic interaction between host and guest, and that the attractions are dominated by the dispersion forces. Generally, the van der Waals terms are between one and two orders of magnitude larger than the electrostatic contributions. Hence the forces most responsible for holding the hydrocarbon complexes together are the short range dispersion forces. The alkyl halide **4** has short-range van der Waals interactions like the

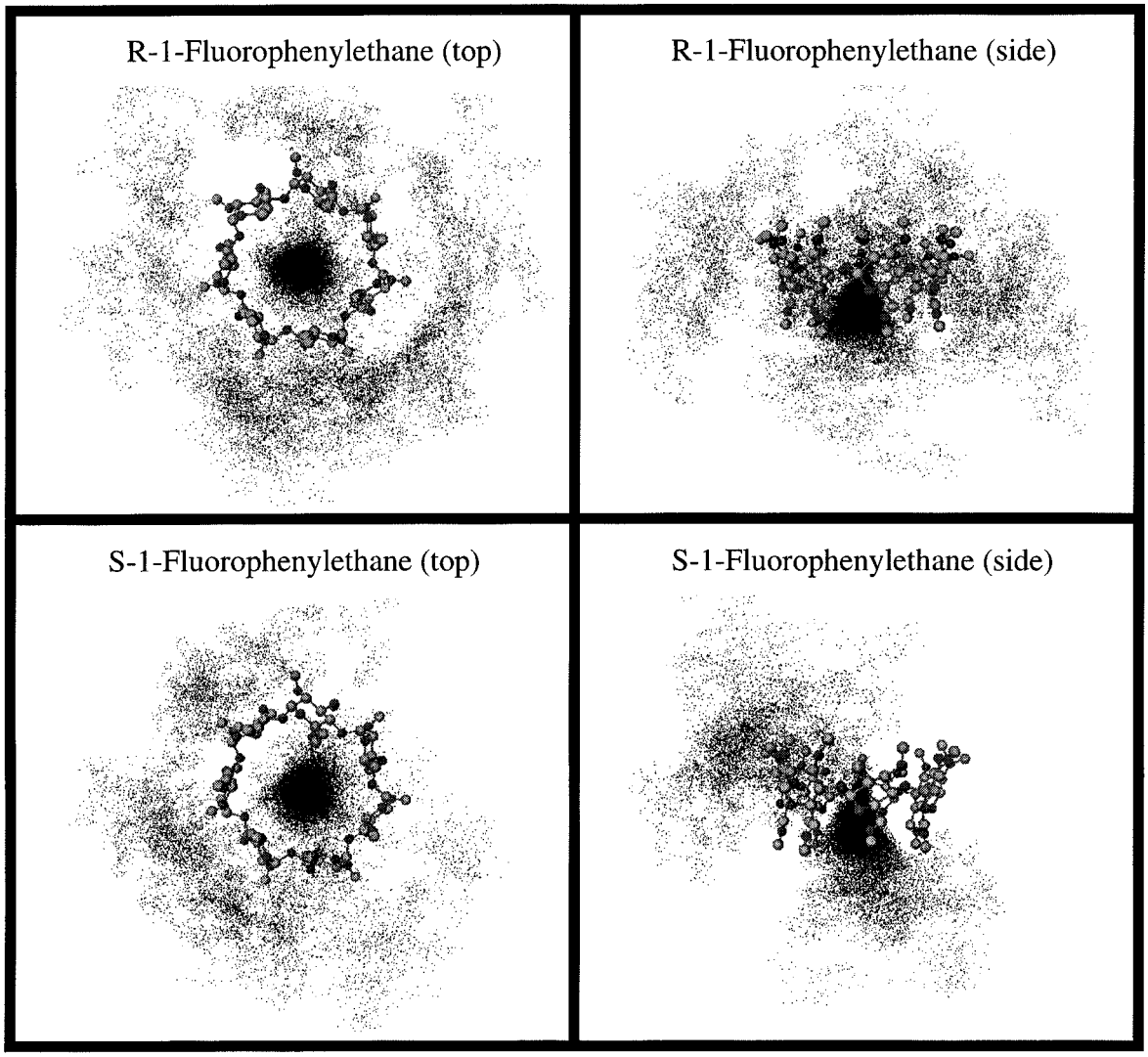

Figure 7. 'Dot plot' illustrating the 1-fluorophenylethane center of mass, relative to the cyclodextrin, over the combined 25 ns simulation. (Top) end-on and side views of the *R* enantiomer; (bottom) end-on and side views of the *S* enantiomer

© 1997 by John Wiley & Sons, Ltd.

Table 4. Trajectory-averaged intermolecular energies for **2**–CD (kJ mol^{-1})

	R		*S*	
Trajectory	vdW	Electrostatic	vdW	Electrostatic
I	−23·39	−0·99	−9·98	−0·53
II	−22·73	−0·66	−10·97	−0·47
III	−11·14	−0·49	−10·60	−0·59
IV	−8·77	−0·27	−8·14	−0·43
V	−11·66	−0·57	−12·98	−0·59
Average	−15·54	−0·60	−10·53	−0·52

hydrocarbons, but is anticipated to have additional long-range electrostatic contributions that may be significant due to the electronegative fluorine. In this case the electrostatic contributions are larger than those for the hydrocarbon complexes but, again, the van der Waals terms dominate the host–guest association. For the three analytes studied here, then, we conclude that while electrostatic and dispersion terms contribute to the intermolecular complexation, the major force holding the complexes together are the short-range dispersion forces.

The next issue we consider is the question of enantioselectivity. In particular we ask if the dispersion forces are more or less discriminating than the electrostatic forces. To answer this, one need only compare the averaged intermolecular van der Waals energies for the *R* enantiomer compared with the *S* enantiomer in Tables 4–6 and determine if those energy differences are greater or less than the corresponding electrostatic values. For example, in Table 4 the average intermolecular van der Waals energy difference is 4·01 kJ mol^{-1} (−15·54 vs −10·53) while the average intermolecular electrostatic difference is only 0.08 kJ mol^{-1} (−0·60 vs −0·52) indicating that the intermolecular van der Waals force is substatially more enantiodiscriminating than the intermolecular electrostatic force. For all the analytes addressed in this study, using this particular force field and the aforementioned sampling strategy, it is seen that the differential van der Waals forces are larger, typically by one to two orders of magnitude, than the electrostatic contributions. This indicates that the intermolecular force responsible for enantioselection is the short-range dispersion force. Hence we find that the same forces responsible for host–guest complexation are also responsible for chiral selectivity.

Table 5. Trajectory-averaged intermolecular energies for **3**–CD (kJ mol^{-1})

	R		*S*	
Trajectory	vdW	Electrostatic	vdW	Electrostatic
I	−9·35	−0·26	−7·45	−0·19
II	−12·90	−0·28	−18·24	−0·37
III	−7·77	−0·20	−7·02	−0·19
IV	−5·80	−0·16	−6·47	−0·21
V	−31·86	−0·65	−10·74	−0·29
Average	−13·54	−0·31	−9·98	−0·25

Table 6. Trajectory-averaged intermolecular energies for **4**–CD (kJ mol^{-1})

	R		*S*	
Trajectory	vdW	Electrostatic	vdW	Electrostatic
I	−28·44	−2·77	−41·01	−3·35
II	−44·35	−4·48	−23·86	−2·97
III	−23·80	−3·35	−43·00	−4·36
IV	−26·32	−2·99	−25·99	−2·79
V	−42·54	−4·61	−43·33	−4·18
Average	−33·09	−3·64	−35·44	−3·53

CONCLUSION

In this study, using stochastic molecular dynamics with the AMBER* force field, we simulated the enantioselective binding of weak and moderately polar analytes with permethylated β-cyclodextrin, the most commonly use chiral stationary phase in gas chromatography. We found that averaging over multiple trajectories, each of which should be very long, is need to predict the correct chromatographic retention orders as well as to replicate the very small differential binding energies of these enantiomeric analytes associating with the cyclodextrin.

From these simulations we found that (1) all molecules prefer binding to the interior rather than the exterior of the macrocyclic host because the flexibility of the macrocycle allows it to collapse around the guest and to maximize the intermolecular van der Waals attractions; (2) a preference exists for analytes to associate with the smaller and more flexible primary rim rather than the wider, secondary rim; (3) the intermolecular forces responsible for host–guest complexation are the short-range dispersion forces; and (4) the intermolecular forces responsible for enantioselection are also the short-range van der Waals forces.

The analytes studied here are moderately polar and they are representative of many such analytes resolved on this popular CSP. Work is in progress to simulate the binding of polar molecules, particularly alcohols capable of forming strong intermolecular hydrogen bonds to the acetal and ether linkages of the macrocyclic host, for comparison with the results obtained from this study. Those results will be reported in the near future.

ACKNOWLEDGMENTS

This work was carried out under the auspices of a grant from the National Science Foundation (CHE 9412512).

© 1997 by John Wiley & Sons, Ltd.

REFERENCES

1. (a) R. W. Souter, *Chromatographic Separations of Stereoisomers.* CRC Press, Boca Raton, FL (1985); (b) M. Zeif and L. Crane (Eds), *Chromatographic Chiral Separations* (*Chromatographic Science Series*, Vol. 40). Marcel Dekker, New York (1987); (c) W. A. König, *The Practice of Enantiomer Separation by Capillary Gas Chromatography.* Hüthig, Heidelberg (1987); (d) W. L. Hinze and D. W. Armstrong (Eds) *Ordered Media in Chemical Separations* (*ACS Symposium Series*, Vol. 342). American Chemical Society, Washington, DC (1987); (e) S. G. Allenmark, *Chromatographic Enantioseparation. Methods and Application.* Ellis Horwood, Chichester (1988); (f) D. Stevenson and I. D. Wilson (Eds), *Chiral Separations.* Plenum Press, New York (1988); (g) W. J. Lough (Ed), *Chiral Liquid Chromatography.* Blackie, Glasgow (1989); (h) D. Stevenson and I. D. Wilson (Eds), *Recent Advances in Chiral Separations.* Plenum Press, New York (1990); (i) S. Ahuja (Ed), *Chiral Separations by Liquid Chromatography* (*ACS Symposium Series*, Vol. 471). American Chemical Society, Washington, DC (1991); (j) G. Subramanian (Ed), *Chiral Separations by Liquid Chromatography.* VCH, Weinheim (1994).
2. For leading references see E. Loza, D. Lola, A. Kemme and J. Freimanis, *J. Chromatogr. A* **708**, 231–243 (1995).
3. I. W. Wainer, *Trends Anal. Chem.* **6**, 125–128 (1987).
4. For reviews, see (a) T. J. Ward and D. W. Armstrong, *J. Liq. Chromatogr.* **9**, 407–411 (1986); (b) J. Martens and R. Bhushan, *Chem. Ztg.* **112**, 367–371 (1988); (c) J. Martens and R. Bhushan, *Int. J. Pep. Protein Res.* **34**, 433–439 (1989); (d) J. Martens and R. Bhushan, *J. Pharm. Biomed. Anal.* **8**, 259–265 (1990); (e) R. Bhushan and S. Joshi, *Biomed. Chromatogr.* **7**, 235–241 (1993).
5. Pertinent discussions can be found in Ref. 1; for additional reviews concerning gas chromatocraphic applications of cyclodextrins, see (a) W. A. König, in *Drug Stereochemistry, Analytical Methods and Pharmacology*, edited by I. W. Wainer, and D. E. Drayer, pp. 113–145. Marcel Dekker, New York (1988). (b) V. Schurig and H.-P. Nowotny, *Angew. Chem., Int. Ed. Engl.* **29**, 939–942 (1990); (c) M. Jung, S. Mayer and V. Schurig, *LC·GC* 458–462 (1994); (d) V. Mani and C. Wooley, *LC·GC* 734–737 (1995).
6. Pertinent discussions can be found throughout Ref. 1; for additional reviews concerning applications of cyclodextrins in liquid chromatography, see (a) D. W. Armstrong, A. Alak, K. Bui, W. DeMond, T. Ward, T. E. Riehl and W. L. Hinze, *J. Inclu. Phenom.* **2**, 533–538 (1984); (b) D. W. Armstrong, *J. Liq. Chromatogr.* **7**, 353–360 (1984); (c) T. E. Beesley, *Am. Lab.* May, 78–81 (1985); (d) T. J. Ward and D. W. Armstrong, *J. Liq. Chromatogr.* **9**, 407–411 (1986); (e) D. W. Armstrong and S. Han, *CRC Critical Rev. Anal. Chem.* **19**, 175–189 (1988); (f) D. Johns, *Am. Lab.* January, 72–77 (1987); (g) D. W. Armstrong, *Anal. Chem.* **59**, 84–90 (1987); (h) C. Pettersson, *Trends Anal. Chem.* **7**, 209–213 (1988); (i) D. W. Armstrong, M. Hilton and L. Coffin, *LC·GC.* 646–651 (1991); (j) N. Husain and I. M. Warner, *Am. Lab.* October, 80–85 (1993).
7. (a) D. W. Armstrong, Y. Tang, T. Ward and M. Nichols, *Anal. Chem.* **65**, 1114–1117 (1993), (b) G. Yi, J. S. Bradshaw, B. E. Rossiter, S. L. Reese, P. Petersson, K. E. Markides and M. Lee, *J. Org. Chem.* **58**, 2561–2565 (1993); (c) G. Yi, W. Li, J. S. Bradshaw, A. Malik and M. Lee, *J. Heterocycl. Chem.* **32**, 1715–1721 (1995).
8. (a) M. R. Eftink, M. L. Andy, K. Bystrom, D. H. Perlmutter and D. S. Kristol, *J. Am. Chem. Soc.* **111**, 6765–6772 (1989); (b) Y. Inoue, T. Hakushi, Y. Liu, L.-H. Tong, B.-J. Shen and D.-S. Jin, *J. Am. Chem. Soc.* **115**, 475–483 (1993); (c) Y. Inoue, Y. Liu, L.-H. Tong, B.-J. Shen and D.-S. Jin, *J. Am. Chem. Soc.* **115**, 10637–10644 (1993); (d) M. V. Rekharsky, F. P. Schwarz, Y. B. Tewari, R. N. Goldberg, M. Tanaka and Y. Yamashoji, *J. Phys. Chem.* **98**, 4098–4106 (1994); (e) M. V. Rekharsky, F. P. Schwarz, Y. B. Tewari and R. N. Goldberg, *J. Phys. Chem.* **98**, 10282–10291 (1994); (e) M. V. Rekharsky, R. N. Goldberg, F. P. Schwarz, Y. B. Tewari, P. D. Ross, Y. Yamashoji and Y. Inoue, *J. Am. Chem. Soc.* **117**, 8830–8842 (1995).
9. R. Breslow, *Acc. Chem. Res.* **28**, 146–153 (1995), and references cited therein.
10. Recent reviews include (a) Yu. A. Zhdanov, Yu E. Alekseev, E. V. Kompantseva and E. N. Vergeychik, *Usp. Khim* **61**, 1025 (1992); *Chem. Abstr.* **117**, 211714h (1992); (b) K. B. Kano, *Bioorganic Chemistry Frontiers*, Vol. 3, pp. 1–23. Springer, Berlin (1993); (c) K. Takahashi and K. Hattori, *J. Inclus. Phenom. Mol. Recognit. Chem.* **17**, 1–15 (1994); (d) M. M. Maheswaran and S. Divakar, *J. Sci. Ind. Res.* **53**, 924–936 (1994).
11. (a) M. L. Bender and M. Komiyama, *Cyclodextrin Chemistry, Reactivity and Structure* (*Concepts in Organic Chemistry*, 6). Springer, New York (1978); (b) W. Saenger, *Angew. Chem., Int. Ed. Engl.* **19**, 344–357 (1980); (c) J. Szejtli, *Cyclodextrins and Their Inclusion Complexes.* Akadémiai Kaidó, Budapest (1982).
12. (a) D. Duchêne (Ed), *Cyclodextrins and Their Industrial Uses.* Editions de Santé, Paris (1987); (b) J. Szejtli, *Cyclodextrin Technology.* Kluwer, Dordrecht (1988); (c) R. B. Friedman (Ed), *Biotechnology of Amylodextrin Oligosaccharides* (*ACS Symposium Series*, Vol. 458). American Chemical Society, Washington, DC (1991).
13. A. Berthod, W. Li and D. W. Armstrong, *Anal. Chem.* **64**, 873–884 (1992).
14. (a) J. P. Bowen and N. L. Allinger, in *Reviews in Computational Chemistry*, edited by K. B. Lipkowitz and D. B. Boyd, Vol. 2. Chapt. 3, pp. 81–98. VCH, New York (1991); (b) U. Dinur and A. T. Hagler, in *Reviews in Computational Chemistry*, edited by K. B. Lipkowitz and D. B. Boyd, Vol. 2, Chapt. 4, pp. 99–164. VCH, New York (1991).
15. This is a modified version of Kollman's original AMBER force field: S. J. Weiner, P. A. Kollman, D. A. Case, U. C. Singh, C. Ghio, G. Alogona, S. Profeta and P. Weiner, *J. Am. Chem. Soc.* **106**, 765–779 (1984).
16. F. Mohamadi, N. G. J. Richards, W. C. Guida, R. Liskamp, C. Caufield, G. Chang, T. Hendrickson and W. C. Still, *J. Comput. Chem.* **11**, 440–456 (1990).
17. T. Schlick, in *Reviews in Computational Chemistry*, edited by K. B. Lipkowitz and D. B. Boyd, Vol. 3, Chapt. 1, pp. 1–72. VCH, New York (1992).
18. W. F. van Gunsteren and H. J. C. Berendsen, *Mol. Simul.* **1**, 173–184 (1988).
19. Several groups have carried out limonene resolutions on this CSP, including (a) V. Schurig and H.-P. Nowotny, *J. Chromatogr.* **441**, 155–163 (1988); (b) V. Schurig, M. Jung, D. Schmalzing, M. Schleimer, J. Duvekot, J. C. Buyten, J. A. Peene and P. Mussche, *J. High Resolut. Chromatogr.* **13**, 470–474 (1990); (c) G. Takeoka, R. A. Flath, T. R. Mon, R. G. Buttery, R. Teranishi, M. Güntert, R. Lautamo and J. Szejtli, *J. High Resolut. Chromatogr.* **13**, 202–206 (1990); (d) C. Askari, U. Hener, H.-G. Schmarr, A. Rapp and A. Mosandl., *Fresenius J. Anal. Chem.* **340**, 768–772 (1991); (e) W. Keim, A. Köhnes,

© 1997 by John Wiley & Sons, Ltd.

W. Meltzow and H. Römer, *J. High Resolut. Chromatogr.* **14**, 507–529 (1991); (f) A. Mosandl, K. Fischer, U. Hener, P. Kreis, K. Rettinger, V. Schubert and H.-G. Schmarr, *J. Agric. Food Chem.* **39**, 1131–1134 (1991); (g) C. Bicchi, G. Artuffo, A. D'Amato, A. Galli and M. Galli, *Chirality* **4**, 125–131 (1992); (h) F. Kobor, K. Angermund and G. Schomburg, *J. High Resolut. Chromatogr.* **16**, 299–311 (1993).

20. Several groups have resolved pinene on this CSP including all the citations in Ref. 19 and R. Reinhardt, A. Steinborn, W. Engewald, K. Anhalt and K. Schulze, *J. Chromatogr. A* **697**, 475–484 (1995).
21. R. Reinhardt, W. Engewald, O. Goj and G. Haufe, *Chromatographia* **39**, 192–199 (1994).
22. K. B. Lipkowitz, *J. Org. Chem.* **56**, 6357–6357 (1991).
23. For leading references, see (a) J. Wang and I. M. Warner *Microchem. J.* 229 (1993); (b) A. Botsi, K. Yannakopoulou, B. Perly and E. Hadjoudis, *J. Org. Chem.* **60**, 4017 (1995); (c) J. Redondo, J. Frigola, A. Torrens and P. Lupón, *Magn. Reson. Chem.* **33**, 104 (1995).

© 1997 by John Wiley & Sons, Ltd.